GaAs under Intense Ultrafast Excitation: Response of the Dielectric Function

Li Huang, J. Paul Callan, Eli N. Glezer, and Eric Mazur

Department of Physics and Division of Engineering and Applied Sciences, Harvard University, 9 Oxford Street, Cambridge, Massachusetts 02138

(Received 21 May 1997)

We used a new broadband spectroscopic technique to measure the dielectric function of GaAs over the spectral range of 1.5–3.5 eV following intense 70-fs laser excitation. The results provide the most detailed information thus far on the electron and lattice dynamics both above and below the fluence threshold for permanent damage, $F_{\text{th}} = 1.0\ \text{kJ/m}^2$. There are three distinct regimes of behavior: lattice heating ($<0.5F_{\text{th}}$), lattice disordering ($0.6–0.8)F_{\text{th}}$, and a semiconductor-to-metal transition ($>0.8F_{\text{th}}$). Below F_{th}, the changes are completely reversible. [S0031-9007(97)04894-1]

PACS numbers: 78.20.Ci, 78.47.+p

Intense femtosecond laser pulses excite a dense electron-hole plasma in a semiconductor, which causes large changes in band structure and can lead to structural transitions [1–11]. Femtosecond laser pulses also allow one to observe the dynamics of the laser-induced transitions. Motivated in part by potential applications in materials processing, optical switching, and optoelectronic devices, considerable effort has been devoted in the past ten years to observing high-density electron dynamics and understanding atomic motion during subpicosecond laser-induced structural transitions [1–11].

The first experiments on femtosecond laser-excited semiconductors measured transient reflectivity, transmission, and second-harmonic generation, and provided evidence of changes in the materials within a few hundred femtoseconds after excitation [1–6]. More recently, direct determination of the dielectric constant [7] and second-order susceptibility [8], which are fundamental optical properties of the material, has shown that the observed changes result mainly from modifications of the band structure.

Several theoretical studies have addressed the electronic and structural response of semiconductors to intense ultrafast excitation. Calculations of the effects of a screened ionic potential and of electron exchange and correlation on the band structure show that the bandgap in GaAs decreases with increasing carrier density [9]. The gap drops to zero when about 10% of the valence electrons are excited. In other studies, the breaking of covalent bonds by the electronic excitation is shown to cause rapid softening of the phonon modes [10]. This softening leads to lattice instability when 10% of the valence electrons are excited. Recent *ab initio* molecular dynamics simulations for silicon show that laser-induced changes in the distribution of bonding electrons cause the lattice to undergo a structural transition within 100 fs [11].

In this Letter we present time-resolved measurements of the dielectric function $\epsilon(\omega)$ of GaAs across the spectral range from the near-infrared to the ultraviolet. In contrast to previous single-frequency optical measurements [1–8], the new data allow us to clearly identify the nature of the changes in the material as a function of time. Our results add new understanding of the electron and lattice dynamics following femtosecond laser excitation and provide detailed information for comparison to theoretical models.

We use a pump-probe technique to measure $\epsilon(\omega)$ with 100 fs temporal resolution over a photon energy range from 1.5 to 3.5 eV. A (100) GaAs sample (Cr doped, $\rho > 7 \times 10^5\ \Omega\ \text{m}$) is excited with a 70 fs, 1.9 eV (635 nm) pump pulse and is probed by a 1.5–3.5 eV (820–350 nm) broadband pulse. The time delay between the pump and probe pulses can be varied. Different frequencies in the probe pulse arrive at the sample at different times. The results presented below are corrected for the measured temporal dispersion of the probe by temporally shifting the data at each frequency.

To determine both the real and imaginary parts of the dielectric function of bulk GaAs, we measure the spectral reflectivity for p-polarized light of 58° and 75°. These angles provide high sensitivity to changes in the dielectric function. The dielectric function is obtained by numerically inverting the Fresnel reflectivity formulas, taking into account the oxide layer which forms on the surface of GaAs in air. The measured dielectric function $\epsilon(\omega)$ of unexcited GaAs shows excellent agreement with the published value of $\epsilon(\omega)$ for GaAs determined from ellipsometric measurements [12].

The response of GaAs to the excitation depends strongly on the incident fluence. Above a threshold $F_{\text{th}} = 1.0\ \text{kJ/m}^2$, we observe permanent damage under an optical microscope. To avoid making measurements on a previously irradiated spot on the sample, we translate the sample between laser shots.

Figure 1 shows the dielectric function of GaAs 500 fs and 4 ps after excitation by a pulse of $0.45F_{\text{th}}$. The error bars correspond to a 5% uncertainty in the reflectivity measurements. The solid and dashed curves in Fig. 1(a) represent the real and imaginary parts of the dielectric function of unpumped GaAs [12]. At a delay of 500 fs, the data display a drop in the real part and a broadening

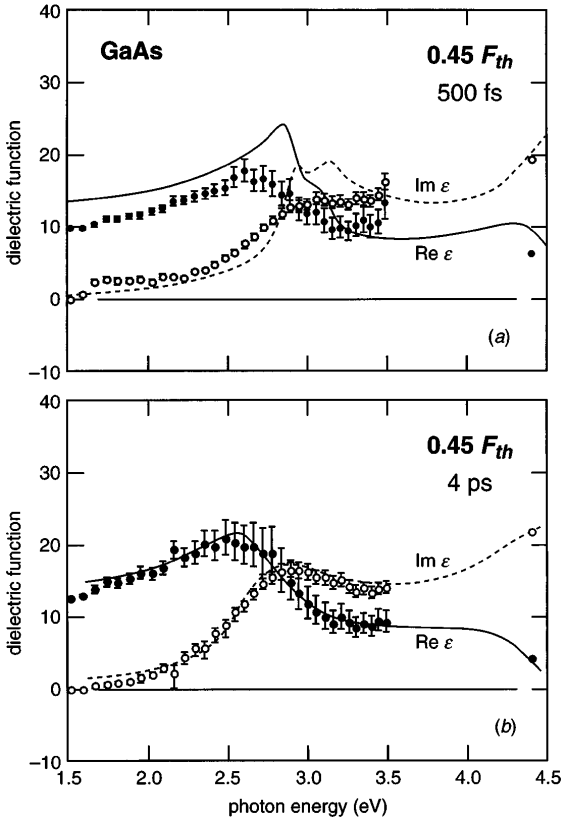

FIG. 1. Dielectric function $\{(\bullet) - \mathrm{Re}[\epsilon(\omega)], (\circ) - \mathrm{Im}[\epsilon(\omega)]\}$ for a pump fluence of $0.45F_{\mathrm{th}}$ after (a) 500 fs and (b) 4 ps. ($F_{\mathrm{th}} = 1.0\ \mathrm{kJ/m^2}$ is the fluence threshold for permanent damage to the sample.) The curves in (a) show the real (solid line) and imaginary (dashed line) parts of the dielectric function for unexcited GaAs [12]. The curves in (b) show the dielectric function for GaAs at 770 K [13].

in the imaginary part of the dielectric function. By 4 ps, $\epsilon(\omega)$ has partly recovered, and agrees well with ellipsometric measurements [13] of the dielectric function of GaAs at 770 K shown by the solid and dashed curves in Fig. 1(b). From 4 ps on, we can fit the data taken at fluences up to $0.5F_{\mathrm{th}}$ with published dielectric functions for GaAs at temperatures up to 780 K [13]. The lattice temperatures obtained from these fits are shown in Fig. 2 as a function of time delay for three different pump fluences. As is to be expected, the lattice temperature increases with increasing fluence. Exponential fits to the data of $0.2F_{\mathrm{th}}$ and $0.35F_{\mathrm{th}}$ yield a rise time of about 7 ps. In the first 2 ps our data cannot be fitted with a dielectric function of heated GaAs, because the dielectric function on this time scale is affected by the excited free carriers and not just by lattice heating.

As shown in Fig. 3, changes in $\epsilon(\omega)$ are much more pronounced at $0.70F_{\mathrm{th}}$. By 4 ps, the imaginary part is broadly spread out while the real part shows a negative slope in frequency across most of the spectral range. The dielectric function resembles that of amorphous GaAs at 300 K [14] [see Fig. 3(b)]; the difference between the data and the curves may be due to heating of the material by

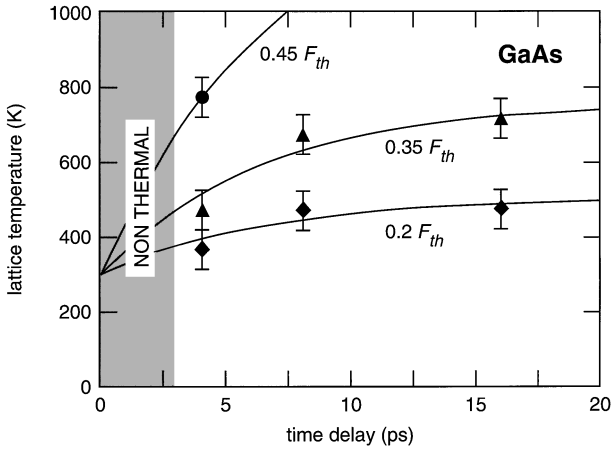

FIG. 2. Lattice heating in the low fluence range. $(\blacklozenge) - 0.2F_{\mathrm{th}}$, $(\blacktriangle) - 0.35F_{\mathrm{th}}$, $(\bullet) - 0.45F_{\mathrm{th}}$. The fitted exponential curves yield a rise time of 7 ps.

the laser excitation. We conclude that the lattice disorders within 4 ps, consistent with our previous measurements of the second-order optical susceptibility, which indicate a reversible loss of long-range order over this fluence range [8].

Above $0.8F_{\mathrm{th}}$, the real part of the dielectric function becomes negative within the observed spectral range, and

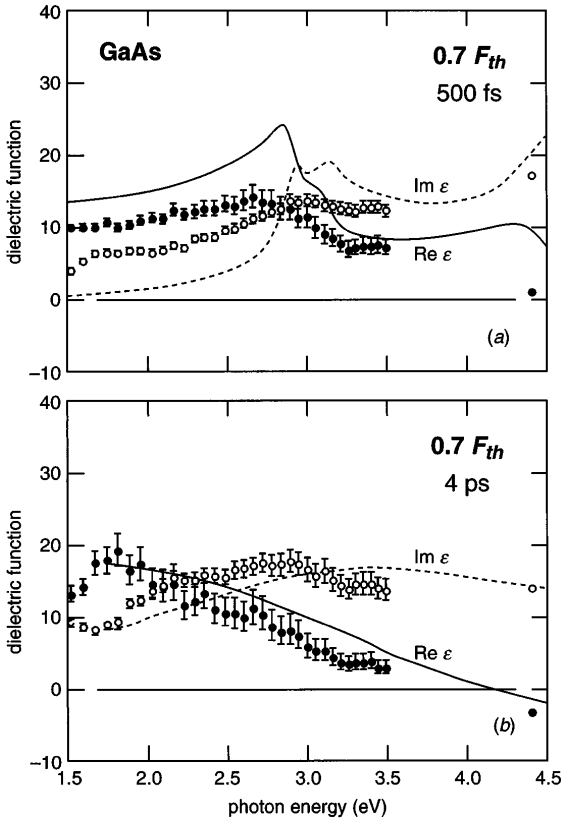

FIG. 3. Dielectric function $\{(\bullet) - \mathrm{Re}[\epsilon(\omega)], (\circ) - \mathrm{Im}[\epsilon(\omega)]\}$ for a pump fluence of $0.7F_{\mathrm{th}}$ after (a) 500 fs and (b) 4 ps. The curves in (a) show the real (solid line) and imaginary (dashed line) parts of $\epsilon(\omega)$ for unexcited GaAs. The curves in (b) show $\epsilon(\omega)$ for amorphous GaAs at room temperature [14].

the zero crossing shifts to lower and lower photon energies at later times. Figure 4 shows $\epsilon(\omega)$ at $1.6F_{\text{th}}$. At 500 fs, the real part is negative above 2.7 eV, indicating that most of the oscillator strength has now moved from an initial value of 4.75 eV [12] to below 2.7 eV. By 4 ps, the zero crossing of the real part has shifted to well below 2 eV. The data below 1.8 eV lie in a region of dielectric function space where the reflectivity is not very sensitive to changes in $\epsilon(\omega)$ and hence the uncertainty in $\epsilon(\omega)$ is large. The curves in Fig. 4(b) show a fit to a Drude model [7,15], yielding a 12 eV plasma frequency and a 0.2 fs free-carrier relaxation time. The large plasma frequency shows that nearly all of the valence electrons in GaAs are behaving as free carriers, indicating that a semiconductor-to-metal transition has occurred. We observe this transition for fluences above $0.8F_{\text{th}}$; the transition occurs faster at higher fluence.

Let us now discuss the physical processes responsible for the observed behavior. Incident photons promote electrons from occupied valence states to empty conduction states, leaving holes behind. A laser pulse of $1.0F_{\text{th}}$ creates a free-carrier density of the order of 10^{22} cm^{-3}, or about 10% of the valence electron density, via linear and nonlinear absorption [15]. The excited free carriers affect

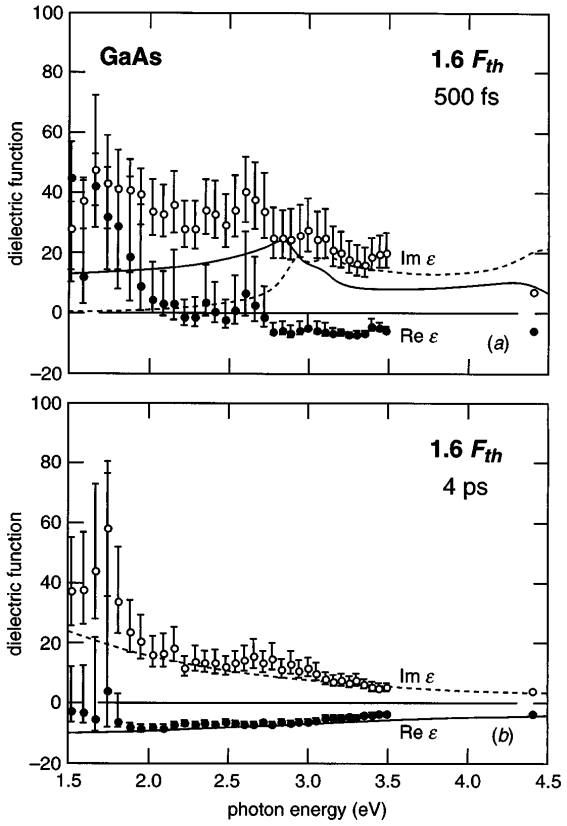

FIG. 4. Dielectric function $\{(\bullet) - \text{Re}[\epsilon(\omega)], (\circ) - \text{Im}[\epsilon(\omega)]\}$ for a pump fluence of $1.6F_{\text{th}}$ after (a) 500 fs and (b) 4 ps. The curves in (a) show the real (solid line) and imaginary (dashed line) parts of $\epsilon(\omega)$ for unexcited GaAs. The curves in (b) show a Drude-model dielectric function with a plasma frequency of 12 eV and a relaxation time of 0.2 fs.

the dielectric function in two ways. First, the free carriers change the dielectric function by free-carrier absorption, as described by the Drude model, resulting in a decrease in the real part and an increase in the imaginary part. Second, screening of the ionic potential due to the free carriers and electron many-body effects change the band structure [9], which, in turn, affects the dielectric function. These free-carrier effects arise immediately after the excitation and dominate the changes in $\epsilon(\omega)$ for several hundred femtoseconds after excitation, before changes in the lattice become important.

Below $0.8F_{\text{th}}$, the changes in the dielectric function, $\Delta\epsilon(\omega)$, at a 500 fs time delay [see, e.g., the difference between the experimental data and the curves in Figs. 1(a) and 3(a)], cannot be accounted for by a Drude contribution to the dielectric function. Below 2.5 eV, the strength and spectral shape of the changes are inconsistent with the Drude model; above 2.5 eV, even the sign of the change in the imaginary part of $\epsilon(\omega)$ does not agree with the Drude model. The observed broadening and downward shift of the absorption peak in the dielectric function are consistent, however, with screening and many-body effects. A recent band-structure calculation for femtosecond laser-excited GaAs shows that screening and many-body effects decrease the direct gaps at the L and X points [9]. Because the direct gaps at the L and X points give rise to absorption peaks in the dielectric function at 3.0 and 4.75 eV [16], the laser-induced decrease in these gaps results in a broadening and downward shift of the absorption peaks, in agreement with the changes we observe.

The free carriers relax through a combination of phonon emission, Auger recombination, radiative recombination, and carrier diffusion. Radiative recombination is a relatively slow process which does not play an important role in the first few picoseconds. Diffusion is important for carrier densities below 10^{19} cm^{-3}, but carrier confinement limits the diffusion rate for carrier densities above 10^{21} cm^{-3} [17]. Our measurements at fluences below $0.5F_{\text{th}}$ indicate that Auger recombination and phonon emission are most important at carrier densities above 10^{21} cm^{-3}: The effects of free carriers on $\epsilon(\omega)$ subside within 4 ps, whereas the lattice heats in 7 ps (cf. Figs. 1 and 2). Rapid Auger recombination reduces the carrier density without affecting the total carrier energy. The average energy per carrier increases, so each remaining carrier emits more phonons to reach the band edge which increases the energy relaxation time. Thus, the carrier density decreases more rapidly than the total carrier energy, consistent with our observations. The lifetime of nonequilibrium LO phonons generated by carrier relaxation [18] may also contribute to the observed lattice heating time; however, its role at high carrier density is not clear because the phonon dynamics are very complex at these densities.

It is important to note that the lattice heating referred to above is different from conventional heating. Conventional heating causes both the expansion of the lattice and increased vibrational motion. On a picosecond time scale,

however, lattice expansion cannot take place. It therefore may appear surprising that the dielectric function following low-fluence femtosecond laser excitation agrees with that of hot GaAs [cf. Fig. 1(b)]. However, it has been suggested that the major contribution to changes in the dielectric function of GaAs heated by conventional means comes from the increased vibrations of the atoms [19], and our measurements support this theory.

In the medium fluence regime ($0.6-0.8F_{\mathrm{th}}$), the dielectric function after several picoseconds cannot be explained simply by lattice heating because the measured $\epsilon(\omega)$ differs from what can be extrapolated based on measurements of $\epsilon(\omega)$ for GaAs at elevated temperatures. Also, the dielectric function does not resemble the metal-like dielectric function of a molten semiconductor, as observed for liquid Si and Ge [20]. Instead, our results indicate that the lattice disorders after a few picoseconds for medium pump fluences [see, e.g., Fig. 3(b)]. Recent theoretical calculations [10] show that intense excitation can disorder the lattice directly by destabilizing the atomic bonds. Indeed, the disordering we observe results directly from the excitation—we do not see a metal-like dielectric function, typical of a molten semiconductor, at any time prior to the observed loss of crystalline order.

In the high fluence regime (above $0.8F_{\mathrm{th}}$), the zero crossing of $\mathrm{Re}[\epsilon(\omega)]$ shifts to lower photon energies with time [cf. Figs. 4(a) and 4(b)], suggesting a decrease in the bonding-antibonding gap. When the minimum gap between the valence and conduction bands falls to zero, a semiconductor-to-metal transition occurs [e.g., Fig. 4(b)]. The observed shift in zero crossing, and hence the decrease in gap, progresses for several picoseconds. If this decrease in gap was due solely to free-carrier effects, the gap would be smallest immediately after the excitation, when the free-carrier density is highest. By contrast, structural changes and their effect on $\epsilon(\omega)$ would develop with time after the excitation, consistent with our experimental observation that the gap decreases for several picoseconds.

As described earlier, theoretical calculations [10] have shown how intense laser excitation can cause nonthermal structural changes. In GaAs, excitation of about 10% of the valence electrons is sufficient to cause a lattice instability and a deformation of the zincblende structure [10]. Other calculations have shown that deformations of the zincblende lattice lead to a band-gap collapse and a semiconductor-to-metal transition [21,22] which would result in dielectric functions such as those we observe at fluences above $0.8F_{\mathrm{th}}$.

In conclusion, we have determined the response of the dielectric function of GaAs to intense femtosecond excitation with 100 fs resolution. The measurements extend from 1.5 to 3.5 eV and provide the most detailed view thus far of the electron and lattice dynamics during a laser-induced phase transition.

The initial response is dominated by changes in band structure caused by the laser-excited free carriers. After several picoseconds, the free-carrier density has decreased and lattice changes dominate the changes in $\epsilon(\omega)$. Below $0.5F_{\mathrm{th}}$, we observe lattice heating with a temperature rise time of about 7 ps, as the carriers transfer their energy to the lattice. In the range $0.6-0.8F_{\mathrm{th}}$, the lattice becomes disordered within 4 ps after excitation. Above $0.8F_{\mathrm{th}}$, we observe a downward shift of the bonding-antibonding splitting which results in a transition to a metal-like state after several picoseconds. The time scale over which the gap decreases suggests that the cause is a structural change arising directly from the excitation. Finally, we note that, below the damage threshold F_{th}, the disordering and semiconductor-to-metal transition are completely reversible.

We thank Professor N. Bloembergen, Professor H. Ehrenreich, Professor E. Kaxiras, Professor C. Klingshirn, and Professor F. Spaepen for many valuable discussions. This work is supported by the Joint Services Electronics Program under Contract No. ONR N0014-89-J-1023 and the Army Research Office under Contract No. DAAH04-95-0370.

[1] C. V. Shank, R. Yen, and C. Hirlimann, Phys. Rev. Lett. **50**, 454 (1983); **51**, 900 (1983).
[2] H. W. K. Tom, G. D. Aumiller, and C. H. Brito-Cruz, Phys. Rev. Lett. **60**, 1438 (1988).
[3] S. V. Govorkov *et al.,* Opt. Lett. **16**, 1013 (1991).
[4] K. Sokolowski-Tinten *et al.,* Appl. Phys. A **53**, 227 (1991).
[5] H. R. Choo *et al.,* Appl. Phys. Lett. **63**, 1507 (1993).
[6] P. N. Saeta *et al.,* Phys. Rev. Lett. **67**, 1023 (1991).
[7] E. N. Glezer *et al.,* Phys. Rev. B **51**, 6959 (1995).
[8] E. N. Glezer *et al.,* Phys. Rev. B **51**, 9589 (1995).
[9] D. H. Kim, H. Ehrenreich, and E. Runge, Solid State Commun. **89**, 119 (1994).
[10] P. Stampfli and K. H. Bennemann, Phys. Rev. B **42**, 7163 (1990); **46**, 10 686 (1992); **49**, 7299 (1994).
[11] P. Silvestrelli *et al.,* Phys. Rev. Lett. **77**, 3149 (1996).
[12] E. D. Palik, in *Handbook of Optical Constants of Solids,* edited by E. D. Palik (Academic, New York, 1985).
[13] H. Yao, P. G. Snyder, and J. A. Woollam, J. Appl. Phys. **70**, 3261 (1991).
[14] M. Erman *et al.,* J. Appl. Phys. **56**, 2664 (1984).
[15] P. N. Saeta, Ph.D. thesis, Harvard University, 1991.
[16] P. Y. Yu and M. Cardona, *Fundamentals of Semiconductors* (Springer, Berlin, 1996).
[17] H. M. van Driel, Phys. Rev. B **35**, 8166 (1987).
[18] D. von der Linde, J. Kuhl, and H. Klingenberg, Phys. Rev. Lett. **44**, 1505 (1980).
[19] G. A. Samara, Phys. Rev. B **27**, 3494 (1983); S. Gopalan, P. Lautenschlager, and M. Cardona, Phys. Rev. B **35**, 5577 (1987).
[20] G. E. Jellison, Jr. and D. H. Lowndes, Appl. Phys. Lett. **51**, 352 (1987).
[21] W. A. Harrison, *Electronic Structure and the Properties of Solids: The Physics of the Chemical Bond* (Dover, New York, 1989).
[22] S. Froyen and M. L. Cohen, Phys. Rev. B **28**, 3258 (1983).